

ChemComm

Accepted Manuscript



This article can be cited before page numbers have been issued, to do this please use: D. Liu, H. Wang, J. Wang, D. Zhong, L. Jiang and T. Lu, *Chem. Commun.*, 2018, DOI: 10.1039/C8CC04892D.



This is an Accepted Manuscript, which has been through the Royal Society of Chemistry peer review process and has been accepted for publication.

Accepted Manuscripts are published online shortly after acceptance, before technical editing, formatting and proof reading. Using this free service, authors can make their results available to the community, in citable form, before we publish the edited article. We will replace this Accepted Manuscript with the edited and formatted Advance Article as soon as it is available.

You can find more information about Accepted Manuscripts in the [author guidelines](#).

Please note that technical editing may introduce minor changes to the text and/or graphics, which may alter content. The journal's standard [Terms & Conditions](#) and the ethical guidelines, outlined in our [author and reviewer resource centre](#), still apply. In no event shall the Royal Society of Chemistry be held responsible for any errors or omissions in this Accepted Manuscript or any consequences arising from the use of any information it contains.



COMMUNICATION

Highly efficient and selective visible-light driven CO₂-to-CO conversion by a Co-based cryptate in H₂O/CH₃CN solution

.Received 00th January 20xx,
Accepted 00th January 20xx

Dong-Cheng Liu,^a Hong-Juan Wang,^b Jia-Wei Wang,^a Di-Chang Zhong,^{*b} Long Jiang,^{*a} and Tong-Bu Lu^{*ab}

DOI: 10.1039/x0xx00000x

www.rsc.org/

Herein, we report a mononuclear Co(II) cryptate which exhibits highly efficient and selective for photocatalytic CO₂-to-CO conversion in H₂O/CH₃CN solution. The TON and selectivity reach as high as 51392 and 98%, respectively.

Converting CO₂ into fuels or chemical feedstock compounds could in principle reduce fossil fuel consumption and CO₂ emissions.¹ Visible-light driven CO₂ reduction is a promising technology for recycling CO₂ back to fuels, which has received much attention in recent years.² A considerable challenge is to develop efficient and selective catalysts, which is a key factor in photocatalytic CO₂ reduction systems. Compared with heterogeneous catalysts,³ homogeneous molecular catalysts are widely used in photocatalytic CO₂ reduction for their advantages in ligand tuning and mechanistic revealing.⁴

In many photocatalytic systems for CO₂ reduction, noble metal complexes (Re,⁵ Ru,⁶ Ir,⁷ etc.) have been frequently studied as homogeneous catalysts.⁸ However, the use of earth-abundant metals for catalyst is desired. Recently, a number of molecular catalysts based on Co,^{2d,9} Ni,^{4a,4d,10} Mn,¹¹ Fe,^{1a,12} and Cu¹³ have been reported. Although great progress has been achieved in CO₂ reduction, most of the reported molecular catalysts display low efficiency and/or selectivity, especially in water-containing systems.^{6b,10a,14} Large scale solar-to-fuel conversion from these systems is not feasible. Fortunately, molecule catalysts have a distinct advantage that their catalytic efficiency can be improved by modifying the chemical structure of ligands as far as they are stable under highly reductive conditions.¹⁵

Recently, our research group have developed a dinuclear cobalt cryptate [Co₂(OH)L](ClO₄)₃ (L = N[(CH₂)₂NHCH₂(m-C₆H₄)CH₂-NH(CH₂)₂]₃N) that can rapidly fix CO₂ within its cavity and act as an

efficient homogeneous catalyst for photocatalytic CO₂-to-CO conversion (TON = 16896, CO selectivity of 98%).^{2d} Such a model is reminiscent of the trapping of substrates within biochemical structures, such as enzyme pockets, the interior of proteasomes, or within the ribosome.¹⁶ Actually, enzymes are the nature's creation of catalysts that provide molecular-sized and -shaped pockets capable of binding substrates and catalyzing unique and efficient reactions under mild conditions.¹⁷ Inspired by this conception, we initially aimed to explore enzyme-like catalysts to accelerate photocatalytic CO₂ reduction. Particularly, we have interest in cryptate-type complexes which not only have structural beauty but also are useful as host molecules with tailorable internal volume, functionality and active metal sites.¹⁸ More importantly, they can bind substrates with the catalytically active sites within their cavities, lowering activation energies and improving catalytic performance. As a result, this class of materials is potentially useful for highly efficient and selective catalysts for photoinduced CO₂ reduction.^{2d,19}

Based on our previous work, herein, we further designed and synthesized a new cryptand (L¹ = N[(CH₂)₂NHCH₂(2,6-C₁₀H₆)CH₂NH(CH₂)₂]₃N) and a tripodal ligand (L² = N[(CH₂)₂NHCH₂(2-C₁₀H₆)]₃), and their corresponding mononuclear cobalt complexes [Co(HL¹)(DMF)](ClO₄)₃ (**1**) and [CoL²(OH)]ClO₄ (**2**) (Fig. 1 and Fig. S1). Consistent with our prediction that cryptate complex **1**, encapsulating the catalytically active Co^{II} center within its cavity, possesses higher catalytic activity than that of the tripodal complex **2** for photocatalytic CO₂-to-CO conversion in a water-containing system, with the TON, TOF and CO selectivity values of 51392, 1.43 s⁻¹ and 98% for **1**, and 30976, 0.86 s⁻¹ and 97% for **2**, respectively. Even under simulated flue-gas (CO₂/Ar = 10/90), **1** still exhibits highly active and selective for photochemical CO₂-to-CO conversion. Control experiments and DFT calculations results demonstrate that the enhanced catalytic activity of **1** can be ascribed to its unique structure, which endows the low reduction potential of the catalytic centre Co^{II} and low energy barrier of the catalytic transition states.

The synthesis and characterization of **1** and **2** were described in the Supporting Information. Single-crystal X-ray diffraction showed that **1** was crystallized in a triclinic space group *P*-1 (Table S1), with the centre metal Co^{II} encapsulated in the cavity and coordinated to

^a MOE Key Laboratory of Bioinorganic and Synthetic Chemistry, School of Chemistry, Sun Yat-Sen University, Guangzhou 510275, China. E-mail: lutongbu@mail.sysu.edu.cn; cesil@mail.sysu.edu.cn

^b Institute of New Energy Materials & Low Carbon Technology, School of Material Science & Engineering, Tianjin University of Technology, Tianjin 300384, China. E-mail: zhong_dichang@hotmail.com

† Footnotes relating to the title and/or authors should appear here.

Electronic Supplementary Information (ESI) available: [details of any supplementary information available should be included here]. See DOI: 10.1039/x0xx00000x

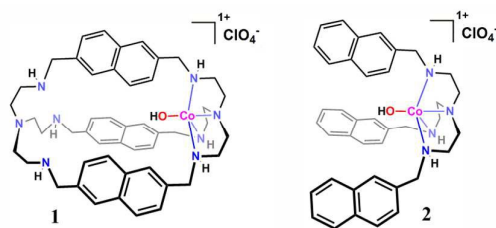


Fig. 1 Chemical structures of **1** and **2**.

five N atoms from one **L**¹ and one DMF molecule (Fig. S1, Table S2). The result of ESI-MS showed that DMF molecule of **1** were replaced by OH⁻ in H₂O/CH₃CN mixed solution (Fig. S2). The photocatalytic experiments for CO₂ reduction was performed in a 5 mL CO₂-saturated H₂O/CH₃CN solution (*v/v* = 1:4) containing a catalyst, a sacrificial reductant TEOA (triethanolamine), and a photosensitizer [Ru(phen)₃](PF₆)₂ (**Ru-PS**), irradiated by a LED light (100 mW cm⁻²). A wavelength of 450 nm was selected as the Ru-PS displays a broad absorption band in the visible region and a maximum peak at 448 nm (Fig. S3). Gas samples were quantified by a gas chromatography. Table 1 summarizes the results of the photocatalytic reactions. After 10 h irradiation, the visible-light photoredox cycle produced 4.22 μmol CO and a by-product H₂ 0.089 μmol in the presence of 0.025 μM of **1**, corresponding to TON and TOF values for CO of 33792 and 0.94 s⁻¹ (Table 1, Entry 1 and Fig. 2), respectively. No formate species was observed in the solution by ion chromatograph. For **2**, 2.33 μmol CO and 0.065 μmol H₂ were detected under the same conditions, corresponding to TON and TOF values for CO of 18656 and 0.52 s⁻¹, respectively (Table 1, Entry 2). These results show that **1** displays higher catalytic activity than **2**. The selectivity to CO of **1** and **2** are 98% and 97%, respectively, indicating that both **1** and **2** exhibit high selectivity for photocatalytic CO₂-to-CO conversion.

Table 1 Photoinduced CO₂-to-CO conversion catalyzed by **1** under various conditions.

Entry	Cat. [μM]	Cat.	CO [μmol]	H ₂ [μmol]	Selectivity to CO	TON for CO	TOF for CO [s ⁻¹]
1	0.025	1	4.22	0.089	98	33792	0.94
2		2	2.33	0.065	97	18656	0.52
3	0	Blank	0	0.047	0	0	0
4			0	0	0	0	0
5	0.025	1	0	0	0	0	0
6			0	0.042	0	0	0
7	0.5	1	1.50	0.071	95	600	0.017
8	1.0	1	7.91	0.23	97	1582	0.04
9	0.0125	1	3.21	0.032	98	51392	1.43

Entry 1: **1** (0.025 μM); Entry 2: **2** (0.025 μM); Entry 3: without catalyst; Entry 4: without **Ru-PS**; Entry 5: without light; Entry 6: without TEOA. Entry 7: 10% CO₂; Entry 8: **1** (1.0 μM); Entry 9: **1** (0.0125 μM). Reaction conditions: TEOA (0.3 M), **Ru-PS** (0.4 mM), 5 mL CO₂-saturated H₂O/CH₃CN solution (*v/v* = 1:4) irradiation for 10 hours by a LED light (450 nm, irradiation area 0.8 cm², 100 mW·cm⁻²), 25 °C. TON and TOF values are averaged over three reactions, all the data with deviations below 5%.

We also studied the effects of other experimental parameters on CO production in this photocatalytic system using **1** as a catalyst. On one hand, no CO was detected in the absence of **1** (Table 1, Entry 3) in the reaction system. In addition, the photocatalysis was investigated using ¹³C-labeled CO₂ and ¹³CO was detected by GC-MS (Fig. S4). These results strongly indicate that CO originated from photoinduced CO₂ reduction. In the control experiments without **Ru-PS**, light and TEOA, all led to no appreciable CO formation (Table 1, Entries, 4-6), demonstrating that all these components in the system are necessary for the CO₂-to-CO conversion. Besides, the concentration dependence of **1** on CO₂ reduction activity was studied under the same conditions, and the results exhibit that the CO amount assume a first-order linear with the concentrations of **1** range from 0 μM to 1.5 μM (Fig. S5), which suggest that the rate-limiting step for CO₂ reduction involves a single Co site.^{4d}

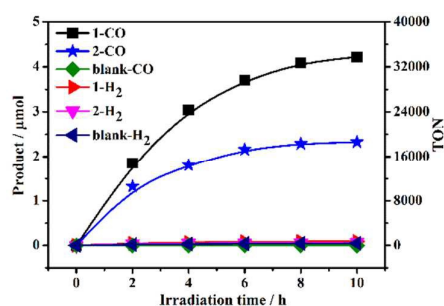


Fig. 2 Time trace of CO and H₂ evolution under irradiation by a LED light ($\lambda = 450$ nm) with 0.025 μM **1** and **2**, 0.3 M TEOA and 0.4 mM Ru(phen)₃(PF₆)₂ in H₂O/CH₃CN solution (*v/v* = 1: 4).

The photocatalytic activities of **1** under different conditions were also investigated. Using 1.0 μM **1**, 7.91 μmol of CO was generated, with the TON of 1582 (Table 1, Entry 8 and Fig. S6). The calculated quantum yield was 0.15%. Besides, reducing the concentration of **1** to 0.0125 μM, the conversion of CO₂ to CO was also achieved. The TON value reached as high as 51392 (Table 1, Entry 9). Meanwhile, **1** exhibits high CO ($\geq 97\%$) in the presence of 1.0 and 0.0125 μM of **1** (Table 1, Entry 8 and 9). These high TONs and selectivity at relatively high and low concentrations further confirm that **1** is an excellent catalyst for photocatalytic CO₂-to-CO conversion. To further test the catalytic performance of **1**, the photocatalytic CO₂ reduction by **1** was also investigated under a low CO₂ concentration like flue gas with 5-15% CO₂²⁰. The results showed that the TON of **1** in 10% CO₂ (Table 1, Entry 7) decreased compared with that obtained in pure CO₂ (Table 1, Entry 1), while the value is still higher than many reported catalysts behaving in pure CO₂.^{2c} Furthermore, in such a low CO₂ concentration, the CO selectivity of **1** reached as high as 95%. Therefore, the high activity and selectivity of **1** behaving under either pure CO₂ or a flue-gas-like atmosphere (10% CO₂) in a water-containing catalytic system establish its promise for potential larger-scale CO production cycles.^{4d}

The durability of a catalyst is an important factor for a photocatalytic CO₂ reduction system. Theoretically, degradation of photosensitizer, catalyst, or sacrificial reductant is attribute to the stagnation of the photocatalytic system. Since TEOA is in large excess in the catalytic system, the inactivation is probably related to

the photo-degradation of catalyst or **Ru-PS**. The absorbance of **1** in H₂O/CH₃CN solution (*v/v* = 1:4) remains almost no change after 10 irradiation with a LED light (Fig. S7). In contrast, **Ru-PS** exhibits obvious hypochromism under the same conditions (Fig. S7). Therefore, we speculated that the stagnation of the reaction system can be due to the degradation of photosensitizer. This was confirmed by consecutive photocatalytic experiments that the addition of fresh equivalent **Ru-PS** (0.4 mM) can reactivate the ceased CO₂-to-CO conversion (Fig. S8). Besides, dynamic light scattering (DLS) results reveal that no nanoparticles formation during photocatalysis. We conclude from all these results that **1** is a durable homogeneous catalyst in this photocatalytic CO₂ reduction system.

To further verify the structure-catalytic activity relationships, the electrochemical properties of **1** and **2** were investigated by cyclic voltammetry (CV) (Fig. S9). The CV of the cryptate **1** exhibits an irreversible reductive process at $E_{1/2} = -0.90$ V versus (vs.) normal hydrogen electrode (NHE, Fig. S10) under an argon atmosphere, which is determined to Co^{II}/Co^I. For comparison, the CV of complex **2** based on the tripodal ligand shows a Co^{II}/Co^I reduction peak at -1.10 V vs. NHE, which is more negative than that of **1**. Besides, both the CVs of **1** and **2** show enhanced currents at $E_{\text{onset}} = -0.68$ V and -0.80 V vs. NHE under a CO₂ atmosphere, respectively, which is indicative of electrocatalysis. Notably, the onset reduction potential of **1** is also more positive than that of **2**. Thus, the enhanced catalytic efficiency of **1** over **2** can be ascribed to its more positive reduction potential and onset reduction potential, which dramatically boosts the process of photocatalytic CO₂ reduction. These electrochemical results of **1** and **2** are in agreement with their photocatalytic performance and in line with our original hypothesis.

To well understand the photoinduced electron transfer in this catalytic system, the quenching experiments of the excited state **Ru-PS*** were performed by addition of **1** or TEOA. At an excitation wavelength of 450 nm, the luminescence at 583 nm of the excited state **Ru-PS*** in the deaerated solution (H₂O/CH₃CN, *v/v* = 1:4) was effectively quenched by **1** with an apparent quenching rate constants (k_q) of 8.57×10^9 M⁻¹ s⁻¹ obtained from Stern–Volmer plot (Fig. S11). However, the excited state **Ru-PS*** can not be quenched by TEOA, because no obvious fluorescent decrease was observed with the addition of TEOA (Fig. S11). Thus, the quenched mode of **Ru-PS*** can be assigned to an oxidatively quenched mechanism.^{4d,9b} **1** exhibits negligible absorbance above 400, while **Ru-PS** shows a distinct broad trap-state emission around 583 nm (Fig. S3). Because of the lack of spectral overlap between the emission of **Ru-PS** and the absorption of **1**, the energy transfer process is impossible to occur, and the intermolecular electron transfer from the excited state **Ru-PS*** to catalysts is therefore responsible for the emission quenching.²¹

The photocatalytic mechanism for the reduction of CO₂ to CO catalyzed by **1** and **2** were further studied by the density functional theory (DFT) calculations. With detailed calculations, two possible catalytic mechanisms were taken into consideration. The optimum pathway for the photocatalytic CO₂-to-CO conversion catalyzed by **1** is presented in Fig. S12(I): (i) **1** binds with CO₂ within the cavity to form [L-Co^{II}(HCO₃)]⁺ (**b**). (ii) **b** undergoes a proton coupled electron transfer process (PCET), and loses a water molecule to yield [L-Co^I(CO₂)]⁺ (**c**). Then, CO₂ in **c** undergoes a reduction process via

transition state **TS1** and generate [L-Co^{III}(CO₂²⁻)]⁺ (**d**). The energy barrier calculated for **1-TS1** is 9.09 kcal/mol (Fig. S13 and S14). (iii) **d** undergoes the second PCET process and generate [L-Co^{II}(COOH)]⁺ (**e**). (iv) The C–OH bond in [L-Co^{II}(COOH)]⁺ is cleaved to yield **f** via the transition state **TS2**, in which Co^{II} binds to CO as well as OH⁻. The total energy barrier calculated for **1-TS2** is 14.58 kcal/mol (Fig. S13 and S14). (v) After the release of CO, the catalyst is renewed and the photocatalytic cycle resume. If the reaction processes catalyzed by **1** follow catalytic mechanism **I** as shown in Fig. S12(II), the energy barrier for CO₂ reduction (**1-TS1**) increases to 17.38 kcal/mol (Fig. S14), which is much higher than that of the proposed pathway **I** (Fig. S14, 9.09 kcal/mol). On the contrary, catalytic mechanism **II** is the optimum pathway for **2** (Fig. S12(III)), because the energy barrier for CO₂ reduction by **2** (**2-TS1**, 6.14 kcal/mol, Fig. S13 and S15) is lower than that of pathway **I** (7.85 kcal/mol, Fig. S15). The order of CO₂ fixation and the first PCET process in these two catalytic mechanisms are different (Fig. S12). In the presence of **Ru-PS**, **2** first undergoes a PCET process, and lose a water molecule to yield [L-Co^I]⁺ (**b**). Then, CO₂ binds to the reduced Co^I metal center forming a Co–CO₂ adduct [L-Co^I(CO₂)]⁺ (**c**). The following PCET process, C–OH bond breaking, and CO release steps of **2** are the same as that of **1**, with the energy barrier of 16.88 kcal/mol for **2-TS2** (Fig. S13 and S15). The proposed mechanism **II** is similar to that reported by Fujita et al.²² and our group.^{13b,23}

On the basis of calculation results, the photocatalytic CO₂-to-CO conversion catalyzed by **1** and **2** are feasible and consistent with the experimental observations. Besides, according to the proposed mechanisms for the photocatalytic CO₂-to-CO conversion, the C–OH bond breaking step in **TS2** is the rate-limited step for the conversion of CO₂ to CO. The calculation results show that the energy barrier of C–O bond cleavage by **1** (14.58 kcal/mol) is lower than that by **2** (16.88 kcal/mol), indicating that **1** encapsulating the active metal center Co^{II} within its cavity is more favorable to the photocatalytic CO₂-to-CO conversion. These observations combining with the control experimental results indicate that **1** with unique structure shows higher catalytic activity for photochemical CO₂-to-CO conversion than **2**.

In summary, we presented here that a Co-based cryptate **1**, encapsulating catalytically active Co^{II} center within its cavity, can serve as an excellent catalyst for CO₂-to-CO conversion driven by visible-light in a water-containing system. The TON and TOF values of **1** are higher than most reported molecular catalysts. The control experiment and DFT calculation results indicate that the high activity and selectivity of **1** behaving under either pure CO₂ or a flue-gas-like atmosphere (10% CO₂) is due to its lower reduction potential of the catalytic Co^{II} center and lower energy barrier of the transition states. We believe that this work will provide new avenues for the development of efficient and selective molecular catalysts for the photocatalytic CO₂ reduction.

This work was financially supported by National Key R&D Program of China (2017YFA0700104) and NSFC (21331007 and 21790052).

Conflicts of interest

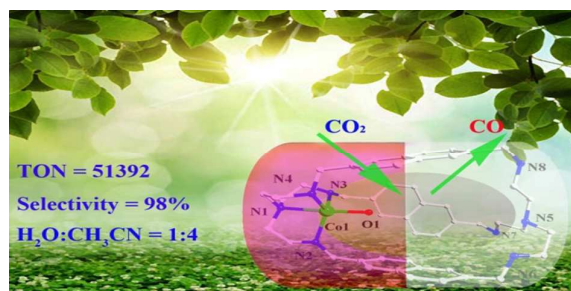
There are no conflicts to declare.

Notes and references

- 1 (a) H. Rao, L. C. Schmidt, J. Bonin and M. Robert, *Nature*, 2017, **548**, 74; (b) J. Hou, S. Cao, Y. Wu, F. Liang, Y. Sun, Z. Lin and L. Sun, *Nano Energy*, 2017, **32**, 359.
- 2 (a) D. Xiang, D. Magana and R. B. Dyer, *J. Am. Chem. Soc.*, 2014, **136**, 14007; (b) A. J. Morris, G. J. Meyer and E. Fujita, *Acc. Chem. Res.*, 2009, **42**, 1983; (c) Y. Yamazaki, H. Takeda and O. Ishitani, *J. Photochem. Photobiol. C*, 2015, **25**, 106; (d) T. Ouyang, H. H. Huang, J. W. Wang, D. C. Zhong and T. B. Lu, *Angew. Chem. Int. Ed.*, 2017, **56**, 738; (e) J. Hou, S. Cao, Y. Wu, Z. Gao, F. Liang, Y. Sun, Z. Lin and L. Sun, *Chem. Eur. J.*, 2017, **23**, 9481.
- 3 (a) R. Kuriki, M. Yamamoto, K. Higuchi, Y. Yamamoto, M. Akatsuka, D. Lu, S. Yagi, T. Yoshida, O. Ishitani and K. Maeda, *Angew. Chem. Int. Ed.*, 2017, **56**, 4867; (b) K. Maeda, R. Kuriki, M. Zhang, X. Wang and O. Ishitani, *J. Mater. Chem. A*, 2014, **2**, 15146; (c) R. Kuriki, K. Sekizawa, O. Ishitani and K. Maeda, *Angew. Chem. Int. Ed.*, 2015, **54**, 2406.
- 4 (a) D. Hong, Y. Tsukakoshi, H. Kotani, T. Ishizuka and T. Kojima, *J. Am. Chem. Soc.*, 2017, **139**, 6538; (b) A. J. Huckaba, E. A. Sharpe and J. H. Delcamp, *Inorg. Chem.*, 2016, **55**, 682; (c) T. Morimoto, C. Nishiura, M. Tanaka, J. Rohacova, Y. Nakagawa, Y. Funada, K. Koike, Y. Yamamoto, S. Shishido, T. Kojima, T. Saeki, T. Ozeki and O. Ishitani, *J. Am. Chem. Soc.*, 2013, **135**, 13266; (d) V. S. Thoi, N. Kornienko, C. G. Margarit, P. Yang and C. J. Chang, *J. Am. Chem. Soc.*, 2013, **135**, 14413.
- 5 (a) X. Qiao, Q. Li, R. N. Schaugaard, B. W. Noffke, Y. Liu, D. Li, L. Liu, K. Raghavachari and L. S. Li, *J. Am. Chem. Soc.*, 2017, **139**, 3934; (b) T. Morimoto, T. Nakajima, S. Sawa, R. Nakanishi, D. Imori and O. Ishitani, *J. Am. Chem. Soc.*, 2013, **135**, 16825; (c) Y. Kou, Y. Nabetani, D. Masui, T. Shimada, S. Takagi, H. Tachibana and H. Inoue, *J. Am. Chem. Soc.*, 2014, **136**, 6021; (d) H. Takeda, K. Koike, H. Inoue and O. Ishitani, *J. Am. Chem. Soc.*, 2008, **130**, 2023.
- 6 (a) K. Kobayashi, T. Kikuchi, S. Kitagawa and K. Tanaka, *Angew. Chem. Int. Ed.*, 2014, **53**, 11813; (b) Y. Kuramochi, M. Kamiya and H. Ishida, *Inorg. Chem.*, 2014, **53**, 3326.
- 7 S. Sato, T. Morikawa, T. Kajino and O. Ishitani, *Angew. Chem. Int. Ed.*, 2013, **52**, 988.
- 8 H. Q. Xu, J. Hu, D. Wang, Z. Li, Q. Zhang, Y. Luo, S. H. Yu and H. L. Jiang, *J. Am. Chem. Soc.*, 2015, **137**, 13440.
- 9 (a) Z. Guo, S. Cheng, C. Cometto, E. Anxolabehere-Mallart, S. M. Ng, C. C. Ko, G. Liu, L. Chen, M. Robert and T. C. Lau, *J. Am. Chem. Soc.*, 2016, **138**, 9413; (b) S. L. Chan, T. L. Lam, C. Yang, S. C. Yan and N. M. Cheng, *Chem. Commun.*, 2015, **51**, 7799; (c) S. Matsuoka, K. Yamamoto, T. Ogata, M. Kusaba, N. Nakashima, E. Fujita and S. Yanagida, *J. Am. Chem. Soc.*, 1993, **115**, 601; (d) J. W. Wang, H. H. Huang, J. K. Sun, T. Ouyang, D. C. Zhong and T. B. Lu, *ChemSusChem*, 2018, **11**, 1025.
- 10 (a) J. L. Grant, K. Goswami, L. O. Spreer, J. W. Otvos and M. Calvin, *J. Chem. Soc. Dalton Trans.*, 1987, 2105; (b) C. Herrero, A. Quaranta, S. El Ghachtouli, B. Vauzeilles, W. Leibl and A. Aukauloo, *Phys. Chem. Chem. Phys.*, 2014, **16**, 12067; (c) J.-W. Wang, W.-J. Liu, D.-C. Zhong and T.-B. Lu, *Coord. Chem. Rev.*, 2017, DOI: 10.1016/j.ccr.2017.12.009.
- 11 (a) P. L. Cheung, C. W. Machan, A. Y. Malkhasian, J. Agarwal and C. P. Kubiak, *Inorg. Chem.*, 2016, **55**, 3192; (b) H. Takeda, H. Koizumi, K. Okamoto and O. Ishitani, *Chem. Commun.*, 2014, **50**, 1491.
- 12 (a) P. G. Alsabeh, A. Rosas-Hernández, E. Barsch, H. Junge, R. Ludwig and M. Beller, *Catal. Sci. Technol.*, 2016, **6**, 3623; (b) H. Takeda, K. Ohashi, A. Sekine and O. Ishitani, *J. Am. Chem. Soc.*, 2016, **138**, 4354; (c) J. Bonin, M. Robert and M. Routier, *J. Am. Chem. Soc.*, 2014, **136**, 16768; (d) H. Rao, J. Bonin and M. Robert, *ChemSusChem*, 2017, **10**, 4447.
- 13 (a) Z. Guo, F. Yu, Y. Yang, C. F. Leung, S. M. Ng, C. C. Ko, C. Cometto, T. C. Lau and M. Robert, *ChemSusChem*, 2017, **10**, 4009; (b) W. J. Liu, H. H. Huang, T. Ouyang, L. Jiang, D. C. Zhong, W. Zhang and T. B. Lu, *Chem. Eur. J.*, 2018, **24**, 4503.
- 14 S. M. Katsura Mochizuki, Ikuyo Takeda, and Takeshi Kondo, *Inorg. Chem.*, 1996, **35**, 5132.
- 15 (a) B. T. Chen, N. Morlanés, E. Adogla, K. Takanahe and V. O. Rodionov, *ACS Catal.*, 2016, **6**, 4647; (b) A. Fihri, V. Artero, M. Razavet, C. Baffert, W. Leibl and M. Fontecave, *Angew. Chem. Int. Ed.*, 2008, **47**, 564; (c) L. Jiao, Y. Wang, H. L. Jiang and Q. Xu, *Adv. Mater.*, 2017, DOI: 10.1002/adma.201703663.
- 16 B. Breiner, J. K. Clegg and J. R. Nitschke, *Chem. Sci.*, 2011, **2**, 51.
- 17 (a) M. Yoshizawa, J. K. Klosterman and M. Fujita, *Angew. Chem. Int. Ed.*, 2009, **48**, 3418; (b) T. S. Koblenz, J. Wassenaar and J. N. Reek, *Chem. Soc. Rev.*, 2008, **37**, 247; (c) A. Natarajan, L. S. Kaanumalle, S. Jockusch, C. L. Gibb, B. C. Gibb, N. J. Turro and V. Ramamurthy, *J. Am. Chem. Soc.*, 2007, **129**, 4132.
- 18 D. J. Tranchemontagne, Z. Ni, M. O'Keeffe and O. M. Yaghi, *Angew. Chem. Int. Ed.*, 2008, **47**, 5136.
- 19 (a) H. G. Hao, X. D. Zheng and T. B. Lu, *Angew. Chem. Int. Ed.*, 2010, **49**, 8148; (b) G. Y. Xie, L. Jiang and T. B. Lu, *Dalton Trans.*, 2013, **42**, 14092; (c) N. C. Baker, N. C. Fletcher, P. N. Horton and M. B. Hursthouse, *Dalton Trans.*, 2012, **41**, 7005; (d) P. K. B. Pradyut Ghosh, Shampa Mandal, Sanjib Ghosh, *J. Am. Chem. Soc.*, 1996, **118**, 1553; (e) M. I. Tohru Koike, Eiichi Kimura, and Motoo Shiro, *J. Am. Chem. Soc.*, 1996, **118**, 3091; (f) J. G.-R. B. G. Cox, and H. Schneider, *J. Am. Chem. Soc.*, 1981, **103**, 1384.
- 20 (a) T. Kajiwara, M. Fujii, M. Tsujimoto, K. Kobayashi, M. Higuchi, K. Tanaka and S. Kitagawa, *Angew. Chem. Int. Ed.*, 2016, **55**, 2697; (b) A. Goeppert, M. Czaun, J. P. Jones, G. K. Surya Prakash and G. A. Olah, *Chem. Soc. Rev.*, 2014, **43**, 7995.
- 21 (a) X. B. Li, Y. J. Gao, Y. Wang, F. Zhan, X. Y. Zhang, Q. Y. Kong, N. J. Zhao, Q. Guo, H. L. Wu, Z. J. Li, Y. Tao, J. P. Zhang, B. Chen, C. H. Tung and L. Z. Wu, *J. Am. Chem. Soc.*, 2017, **139**, 4789; (b) H. Lv, J. Song, H. Zhu, Y. V. Geletii, J. Bacsa, C. Zhao, T. Lian, D. G. Musaev and C. L. Hill, *J. Catal.*, 2013, **307**, 48; (c) M. Zhu, Y. Du, P. Yang and X. Wang, *Catal. Sci. Technol.*, 2013, **3**, 2295.
- 22 (a) E. Fujita, and Van Eldik, Rudi, *Inorg. Chem.*, 1998, **37**, 360; (b) E. Fujita, L. R. Furenlid and M. W. Renner, *J. Am. Chem. Soc.*, 1997, **119**, 4549; (c) T. Ogata, S. Yanagida, B. S. Brunschwig and E. Fujita, *J. Am. Chem. Soc.*, 1995, **117**, 6708; (d) E. Fujita, C. Creutz, N. Sutin and D. J. Szalda, *J. Am. Chem. Soc.*, 1991, **113**, 343.
- 23 T. Ouyang, C. Hou, J. W. Wang, W. J. Liu, D. C. Zhong, Z. F. Ke and T. B. Lu, *Inorg. Chem.*, 2017, **56**, 7307.

Chem Commun

COMMUNICATION



A Co-based cryptate exhibits highly efficient and selective for photocatalytic CO₂-to-CO conversion under either pure CO₂ or 10% CO₂ in water-containing system.